

Crystal structure of an NK cell immunoglobulin-like receptor in complex with its class I MHC ligand

Jeffrey C. Boyington*, Shawn A. Motyka†, Peter Schuck‡, Andrew G. Brooks§ & Peter D. Sun*

* Structural Biology Section, Laboratory of Immunogenetics, National Institute of Allergy and Infectious Diseases, National Institutes of Health, 12441 Parklawn Drive, Rockville, Maryland 20852, USA

† Biochemistry, Cellular and Molecular Biology Program, Johns Hopkins University School of Medicine, 725 N. Wolfe St., Baltimore, Maryland 21205-2185, USA

‡ Bioengineering and Physical Science Program, National Institutes of Health, 9000 Rockville Pike, Bethesda, Maryland 20892-5766, USA

§ Department of Microbiology and Immunology, University of Melbourne, Royal Parade, Parkville, 3052 Victoria, Australia

Target cell lysis is regulated by natural killer (NK) cell receptors that recognize class I MHC molecules. Here we report the crystal structure of the human immunoglobulin-like NK cell receptor KIR2DL2 in complex with its class I ligand HLA-Cw3 and peptide. KIR binds in a nearly orthogonal orientation across the $\alpha 1$ and $\alpha 2$ helices of Cw3 and directly contacts positions 7 and 8 of the peptide. No significant conformational changes in KIR occur on complex formation. The receptor footprint on HLA overlaps with but is distinct from that of the T-cell receptor. Charge complementarity dominates the KIR/HLA interface and mutations that disrupt interface salt bridges substantially diminish binding. Most contacts in the complex are between KIR and conserved HLA-C residues, but a hydrogen bond between Lys 44 of KIR2DL2 and Asn 80 of Cw3 confers the allotype specificity. KIR contact requires position 8 of the peptide to be a residue smaller than valine. A second KIR/HLA interface produced an ordered receptor–ligand aggregation in the crystal which may resemble receptor clustering during immune synapse formation.

Natural killer (NK) cells constitute a vital part of the innate immune system^{1,2}. Like cytotoxic T-cells, NK cells express surface receptors that interact with polymorphic class I MHC molecules and regulate cell lysis. In contrast to T-cell receptor (TCR)/MHC-mediated cellular activation, recognition of class I molecules by NK cells can result in either target cell lysis or the inhibition of lysis depending on whether the receptor contains a charged transmembrane residue that interacts with the immunoreceptor tyrosine-based activation (ITAM) motif containing DAP-12 (ref. 3) or with a cytoplasmic immunoreceptor tyrosine-based inhibitory (ITIM) motif. Furthermore, MHC recognition by NK cell receptors is less allele specific and less peptide dependent. Of particular interest are inhibitory NK cell receptors that protect target cells bearing certain class I MHC allotypes from NK-mediated lysis⁴. Cells that have lost class I MHC expression such as certain tumour or virus-infected cells will not be engaged by inhibitory receptors and consequently may become susceptible to NK cell lysis⁵. The two structurally distinct superfamilies of NK cell receptors are the immunoglobulin-like and the C-type lectin-like receptors (CTLR). To date, the crystal structures of three killer cell immunoglobulin-like (KIR) receptors, KIR2DL1, 2DL2 and 2DL3, and two CTLR receptors, human CD94 and murine Ly49A in complex with H-2D^d, have been determined^{6–10}.

Previous studies indicated that class I HLA recognition by KIR depends on residues 77 and 80 of the class I HLA heavy chain and peptide residues 7 and 8 (ref. 11). The inhibitory receptor KIR2DL2 interacts with the Ser 77 and Asn 80 bearing HLA-Cw1, 3, 7 and 8 allotypes; however, other residues on the HLA molecule must also contribute to the recognition by KIR, because many HLA-B alleles with the same Ser 77 and Asn 80 as HLA-Cw3 are not recognized by KIR2DL2. Receptor mutagenesis has shown that residues 44, 45 and 70 influence class I HLA binding^{11–13}. These studies and the crystal structure of KIR2DL2 have suggested a putative ligand-binding region on the receptor⁷. We now report the crystal structure of KIR2DL2 bound to HLA-Cw3 and provide a molecular mechanism for the allotypic specificity and peptide recognition by KIR molecules on human NK cells. This also reveals a different binding

mode for KIR2DL2 from that of the murine C-type lectin-like receptor Ly49 with its class I ligand H-2D^d despite their functional similarity¹⁰.

Overall structure of the complex

The structure of KIR2DL2 in complex with HLA-Cw3 and the peptide GAVDPLLAL (GAV) was determined by molecular replacement methods and refined to 3.0 Å resolution. The final *R* factors are 23.1% and 29.4% for *R*_{cryst} and *R*_{free}, respectively (Table 1). Each asymmetric unit contains two KIR (KIR A and KIR B) and one HLA-Cw3 molecule. The electron density is continuous in the final

Table 1 Statistics for data collection and refinement

Data collection	
Space group	<i>P</i> 2 ₁ 2 ₁
Cell dimensions	<i>a</i> = 68.5, <i>b</i> = 90.3, <i>c</i> = 207.3 Å
Resolution limit	3.0 Å
Unique reflections	24,517 (1976)*
Redundancy	4.2 (2.2)*
Completeness (%)	92.1 (75.4)*
<i>R</i> _{sym} (%)†	7.3 (32.7)*
<i>I</i> / σ _{<i>I</i>}	15.6 (2.0)*
Refinement (10.0–3.0 Å, <i>F</i> / σ _{<i>F</i>} \geq 1.0)	
No. reflections	21,717
No. nonhydrogen atoms	6411
Solvent molecules	185
<i>R</i> _{cryst} (%)	23.1 (23.4)‡
<i>R</i> _{free} (%)§	29.4 (29.9)‡
Mean B-factor (Å ²)	63.5
Wilson plot B-factor (Å ²)	63.7
r.m.s. deviation from ideality	
Bonds (Å)	0.008
Angles (°)	1.47

* Values for the highest resolution shell (3.11–3.0 Å).

† $R_{sym} = 100 \times \sum |I_h - \langle I_h \rangle| / \sum I_h$, where $\langle I_h \rangle$ is the mean intensity of multiple measurements of symmetry related reflections.

‡ Calculated using all *F* > 0.

§ Five per cent of the reflections were used as a test set for calculating *R*_{free}.

|| Mean B-factors (Å²) for individual domains are HLA-Cw3; $\alpha 1$: 58.2; $\alpha 2$: 58.2; $\alpha 3$: 68.9; $\beta 2m$: 70.1; GAV: 47.4; KIR A: D1, 50.5; D2, 60.5; KIR B: D1, 71.1; D2, 73.5; H₂O: 52.4.

$2F_o - F_c$ map throughout the complex except for four KIR surface loops (residues 143–145 of KIR A and residues 58, 121 and 158–159 of KIR B) located in regions away from the HLA interface. Only KIR A interacts with HLA-Cw3 (Fig. 1). KIR B is situated on the distal end of the D2 domain of KIR A, providing lattice contacts between symmetry related receptors in the crystal. Thus the stoichiometry of KIR:HLA binding is 1:1 in the crystal. This is also supported by analytical equilibrium centrifugation experiments in which the dissociation constant (K_d) for KIR2DL2 and HLA-Cw3 association was measured as 17 μ M and sedimentation curves were best described by a 1:1 interaction model (data not shown).

KIR A interacts with HLA-Cw3 through surface loops near its interdomain hinge region. The binding site for KIR is located

toward the carboxy-terminal end of the peptide and the corresponding region of the $\alpha 1$ and $\alpha 2$ helices. The orientation of the KIR is such that its amino-terminal D1 domain interacts with polymorphic regions of the $\alpha 1$ helix, residues 69–84, and its D2 domain interacts with more conserved regions of the $\alpha 2$ helix, residues 145–151. This produces a nearly orthogonal (88°) docking of KIR to its class I ligand and permits direct contact between KIR and residues 7 and 8 of the GAV peptide.

The structure of KIR2DL2

KIR A is nearly identical to KIR B and to the structure of ligand free KIR with root-mean-square (r.m.s.) differences of 1.04 Å (194 C α pairs) and 0.97 Å (191 C α pairs), respectively⁷. The electron density for KIR A is better than for the unligated KIR B. The hinge angle between the D1 and D2 domains of KIR A, KIR B and free KIR are 81° , 85° and 84° , respectively⁷. Binding of KIR A to HLA-Cw3 results in the displacement of CC' loop residues Lys 44 and Phe 45 by 2.6 Å relative to KIR B and a small change in the interdomain hinge angle. No other significant conformational differences were observed between the HLA-Cw3 contacting loops of KIR A and the corresponding loops of KIR B and free KIR. KIR B is positioned atop the D2 domain of KIR A, burying 710 Å² of surface area (Fig. 1). The biological relevance of this KIR A/KIR B interaction is, however, not clear.

The structure of HLA-Cw3

The overall structure of HLA-Cw0304 displays the salient features of other classical class I MHC molecules, except for subtle differences in the relative orientations of the $\alpha 1\alpha 2$, $\alpha 3$ and $\beta 2m$ domains. Hinge angles between the $\alpha 1\alpha 2$ and $\alpha 3$ domains in class I molecules vary from 55 to 84° , with most between 76 and 80° . The structure of HLA-Cw3 has a nearly orthogonal 87° hinge angle. The $\alpha 1\alpha 2$ domains of HLA-Cw3 and HLA-Cw4 share r.m.s. differences of 0.82 Å (181 C α pairs). The most visible differences are in three variable surface loops of the $\alpha 1\alpha 2$ domain (14–20, 39–44 and 104–107) and in the width of the peptide-binding groove¹⁴. The peptide-binding cleft of HLA-Cw3 near the regions of $\alpha 1$ residues 70–77 and $\alpha 2$ residues 144–152 is ~ 2.5 Å narrower than that of Cw4, but is

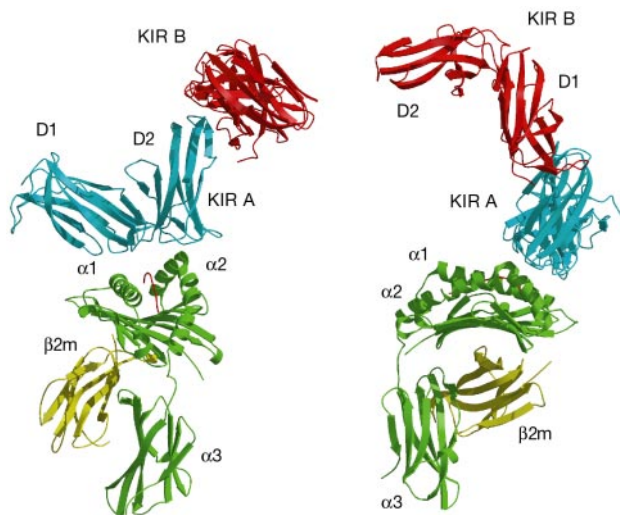


Figure 1 Ribbon drawing showing two views of HLA-Cw3 bound to KIR2DL2. The $\beta 2m$ domain, HLA-Cw3 heavy chain and peptide are yellow, green and magenta, respectively. The KIR molecule bound to HLA-Cw3 and the second KIR molecule are blue and red, respectively. Right view is rotated $\sim 90^\circ$ from left view along the vertical axis. All figures were created using the programs MOLSCRIPT⁴¹, RASTER3D⁴² and GRASP⁴³.

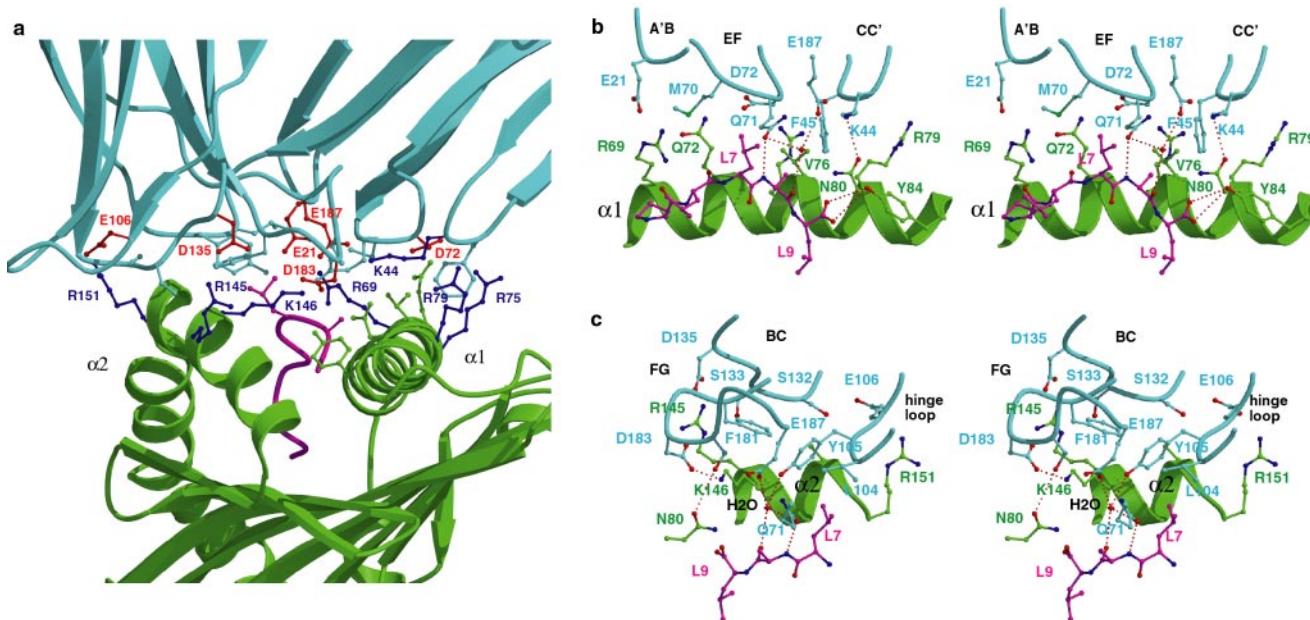


Figure 2 The KIR2DL2/HLA-Cw3 interface. **a**, Charge complementarity at the interface. Basic residues are dark blue, acidic residues are red, and the remaining residues are coloured by molecule. **b,c**, Stereo view of the interaction between domain D1 of KIR, the GAV peptide and the $\alpha 1$ helix of HLA-Cw3 (**b**), and domain D2 of KIR, the hinge loop, the

GAV peptide and the $\alpha 2$ helix of HLA-Cw3 (**c**). KIR is shown in light blue, the GAV peptide in purple and HLA-Cw3 in green. Selected hydrogen bonds are represented by dotted lines.

comparable to that of most other human and mouse class I MHC molecules.

The KIR/HLA interface and its charge complementarity

KIR2DL2 and HLA-Cw3 complex formation buries a total of 1,562 Å², with a predominance of charged and hydrophilic residues at the interface forming an extensive array of hydrogen bonds and salt bridges. The interface is relatively flat with poor shape complementarity (mean shape correlation statistic¹⁵ of 0.58), comparable to those of TCR/MHC, and the CD2–CD58 adhesion complex, but less than those of antibody–antigen interfaces^{16,17}. However, the KIR/HLA interface possesses strong charge complementarity. The interface region on KIR contains one basic (Lys 44) and six acidic residues (Glu 21, Asp 72, Glu 106, Asp 135, Asp 183 and Glu 187), whereas the complementary site on HLA-Cw3 has six basic (Arg 69, Arg 75, Arg 79, Arg 145, Lys 146 and Arg 151) and no acidic residues (Fig. 2a). This results in the formation of four salt bridges between KIR and HLA-Cw3 (Glu 21–Arg 69, Glu 106–Arg 151, Asp 135–Arg 145 and Asp 183–Lys 146). In addition there are eight hydrogen bonds at the interface (Table 2). The charged side chains are evenly distributed over both the KIR and HLA-Cw3 binding sites rather than forming clusters. Each of the six binding loops on KIR has one or more charged residues and the α1 and α2 helices on HLA-Cw3 each have three basic residues in the binding region.

To assess the importance of these interface charge–charge interactions in KIR/HLA recognition, three of the four salt bridges were mutated individually on KIR2DL2. The effect of these single salt-bridge mutations, E106A, D135H and D183A, on HLA-Cw3 binding was measured using surface plasmon resonance (SPR) techniques. As controls, an R33A mutation, well outside the KIR/HLA interface, and a K44M mutation were also created. While the *K_d* of R33A is essentially identical to that of wild-type KIR2DL2, the HLA binding affinity of E106A is reduced by 6-fold and affinities of D135H and D183A are each 20-fold lower than that of the wild type (Table 3). The K44M mutation resulted in a near complete loss of HLA-Cw3 binding, consistent with previous results obtained from cell-surface binding assays¹². The necessity of these salt bridges for successful KIR/HLA recognition emphasizes the crucial role of charge in

HLA recognition and reveals their low tolerance to interface mutations. This suggests a mechanism for the relatively low-affinity KIR receptors to achieve their ligand specificity by requiring a high binding energy threshold for recognition. In contrast, the haematopoietic receptors are more tolerant of mutations.

In total, six loops from KIR interact with the HLA-Cw3/GAV molecule. They include loops A'B (20–23, connecting β-strands A' and B), CC' (43–46) and EF (67–74) of the D1 domain, the hinge loop (103–108), and loops BC (130–135) and FG (182–184) of the D2 domain. Loops A'B, CC' and EF of the D1 domain contact the α1 helix of HLA-Cw3 and the backbone of the GAV peptide with Glu 21 of KIR forming a salt bridge to Arg 69 of HLA-Cw3 (Fig. 2b). Lys 44 from the KIR CC' loop forms a hydrogen bond with Asn 80 of HLA-Cw3. Both residues have been shown to be pivotal in allotypic recognition^{12,18}. A direct hydrogen bond is formed between Gln 71 (Oε1) of the EF loop in KIR and the amide nitrogen of residue Ala 8 in the GAV peptide. This results in close contact between the peptide Ala 8 Cβ atom and the Cδ atom of Gln 71. One of two clusters of nonpolar interactions at the KIR/HLA interface is centred around Val 76 on the α1 helix of HLA-Cw3 and Phe 45 on the CC' loops of KIR. Included in this cluster are the aliphatic portions of Arg 69, Arg 75 and Arg 79 of HLA-Cw3 and Lys 44, Met 70, Gln 71 and Asp 72 of KIR. A simple mutation of Phe 45 to tyrosine (naturally present in the non-inhibitory receptor, KIR2DS2) significantly reduced the affinity of KIR for HLA-Cw3 (ref. 11). The tip of the Phe 45 is only 3.2 Å from the Cβ of Arg 79 in the α1 helix of HLA-Cw3, leaving little space to accommodate an additional hydroxyl group.

The hinge loop and the BC and FG loops of the D2 domain of KIR each form a salt bridge with basic residues (Arg 151, Arg 145 and Lys 146, respectively) on the α2 helix of HLA-Cw3 (Table 2, Fig. 2c). Tyr 105 and Phe 181 together with HLA-Cw3 residues Ala 150 and Lys 146 (aliphatic portion) and Leu 7 of GAV form the second hydrophobic cluster at the interface. In addition, Gln 71, Tyr 105 and Glu 187 of KIR form water-mediated (HOH 38) hydrogen bonds with the carbonyl oxygen of Ala 8 of GAV. The mutation of Tyr 105 to alanine resulted in a 20-fold decrease in HLA-Cw3 binding affinity (Table 3). This mutation presumably destabilized the interface hydrophobic packing. Notably, KIR2DL2 uses the

Table 2 Interactions between KIR2DL2 and HLA-Cw3/GAV

KIR2DL2		HLA-Cw3/GAV		Distance (Å)
Hydrogen bonds* and salt bridges				
Glu 21	Oε1	Arg 69	NH2	3.2
Glu 21	Oε2	Arg 69	NH2	3.2
Lys 44	Nζ	Asn 80	Oδ1	3.3
	O	Arg 79	Nε	3.4
Gln 71	Oε1	Ala 8‡	N	3.4
Asp 72	Oδ2	Gln 72	Nε2	3.4
Glu 106	N	Ala 149	O	2.9
	Oε2	Arg 151	NH2	2.7
Ser 133	O	Arg 145	NH2	2.8
	Oγ	Arg 145	Nε	2.9
	Oγ	Arg 145	NH2	3.2
Asp 135	Oδ2	Arg 145	NH2	2.6
Asp 183	Oδ2	Lys 146	Nζ	2.5
Hydrophobic contact†				
Phe 45	Arg 75(6), Val 76(5), Arg 79(4)			
Met 70	Arg 69(1)			
Gln 71	Val 76(1), Ala 8‡(1)			
Asp 72	Val 76(1)			
Leu 104	Leu 7‡(2)			
Tyr 105	Ala 150(1), Lys 146(3), Leu 7‡(2)			
Ser 132	Ala 149(1)			
Phe 181	Lys 146(8)			
Asp 183	Lys 146(1)			

* Acceptor–donor distances 2.5–3.4 Å.

† Carbon–carbon contacts ≤4.0 Å. Parentheses indicate the number of contacts between a particular residue pair.

‡ GAV peptide residue.

Table 3 Peptide and receptor mutation effects in KIR2DL2/HLA-Cw3 association

Effects of peptide variation in KIR/HLA binding			
Peptide		<i>K_d</i> (μM)	w6/32 binding (%)
GAVDPLLLAL	(GAV)	9.5	100
-----S-	(GAV_S)	42.3	147
-----V-	(GAV_V)	525	130
-----Y-	(GAV_Y)	>600	130
-----K-	(GAV_K)	>600	139
AAADAAAAL	(AAA)	48.5	149
TAMDVVYAL	(TAM)	38	138
QAISPRTL	(QAI)	74	38
HLA-E		>600	84
Effects of amino acid substitutions in KIR/HLA association			
KIR mutant		<i>K_d</i> (μM)	
Wild type		28	
R33A		30	
K44M		>400	
Y105A		>400	
E106A		185	
D135H		>400	
D183A		>400	

For the peptide variation measurements, soluble KIR2DL2 receptor and w6/32 were immobilized on CM5 sensor chips. Binding was measured with a serial dilution of HLA-Cw3 from 0.3 to 40 μM and the dissociation constant *K_d* was determined by a steady-state model for all peptides. The w6/32 binding, listed as the percentage of the HLA-Cw3/GAV binding, was determined using a 9.3 μM concentration of various HLA peptide complexes. The measurements on mutational KIR/HLA association were done similarly with immobilized KIR mutants and a serial dilution for HLA-Cw3/GAV as the analyte.

same six binding loops as do the topologically similar haematopoietic receptors. Unlike the haematopoietic receptors, which interact with their ligands as dimers and have larger hinge angles of 90° or more, the KIR receptor binds to HLA-Cw3 in a 1:1 stoichiometry.

The interface area between KIR and HLA-Cw3 (1,562 Å²) is similar to that observed in TCR/MHC complexes (1,700–1,880 Å²). Furthermore, the two receptors share similar docking orientations (Fig. 3a). There are, however, distinct differences in their recognition of class I MHC antigens. First, the footprint of KIR on HLA-Cw3 is distinct from that of TCR (Fig. 3b, c). The KIR-binding site is centred near the C-terminal P7 and P8 positions of the peptide whereas the known TCR/MHC interfaces are centred near the middle P4–P6 positions of their peptides (Fig. 3b). Their footprints, do, however, overlap partially, suggesting that there is a mutually exclusive binding between KIR and TCR on the same HLA molecule. Second, the ligand-binding domains of KIR (D1 and D2) are two tandem Ig-like domains, whereas the analogous V α and V β domains of TCR are on different chains. Last, unlike TCR/MHC interactions, the KIR/MHC interactions appear to be dominated by charge–charge interactions, that more closely resemble the interaction between the adhesion molecules CD2 and CD58 (ref. 17).

Peptide binding and a potential induced-fit mechanism

The nonamer GAV peptide is derived from the human importin- α -1 subunit (residues 204–212). Its binding to HLA-Cw3 displays characteristics of the classical MHC class I peptide-binding mode in which both termini are securely anchored by a conserved pattern of hydrogen bonds and the middle residues form an arch above the floor of the cleft (Fig. 4a). Side chains from three of the nine residues, P4, P7 and P8, point out of the binding cleft. Of the other six residues, five of them, P1, P2, P3, P5 and P9, are at least 90% buried and P6 is 72% buried. The dimorphic positions Ser 77 and Asn 80 hydrogen bond with the P9 amide nitrogen and carboxylate, respectively. One feature notably missing in HLA-Cw3 as compared with HLA-Cw4 and other class I molecules is a conserved hydrogen bond between Lys 146 and the P9 carboxylate. Instead, Lys 146 of HLA-Cw3 forms a salt bridge with KIR residue Asp 183. A tyrosine in place of serine at position 9 of HLA-Cw3 significantly restricts the size of the P2 pocket, rendering it more similar to HLA-A2 than to HLA-Cw4. As a result, the P2 pocket favours alanine in HLA-Cw3 (refs 19, 20) and tyrosine in HLA-Cw4 (ref. 14).

The most unusual peptide conformation occurs at the position 7 of the peptide. Although P7 in most other known class I MHC nonamer structures has a slightly downward and mainly buried

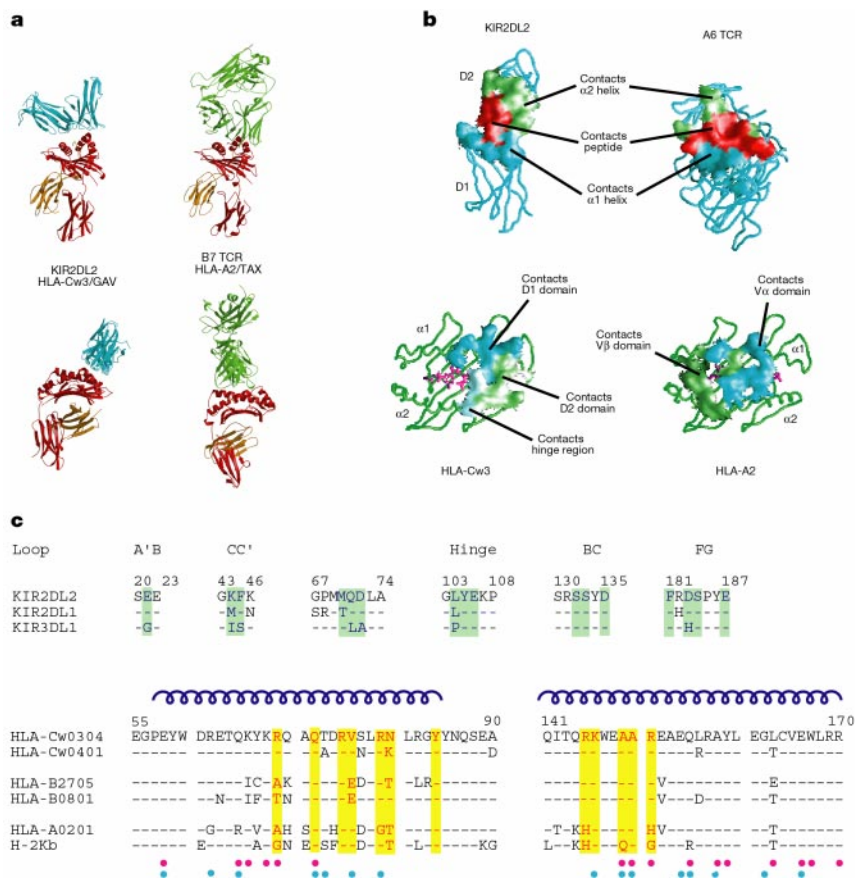


Figure 3 Comparison of KIR/HLA-Cw3 and TCR/MHC interactions. **a**, Docking orientations of KIR2DL2 (left) and A6 TCR (right, PDB accession code 1BD2) onto their class I MHC ligands. The bottom view is orthogonal to the top view. **b**, Worm representations of KIR2DL2 (top left), HLA-Cw3 (bottom left), the A6 TCR (top right, PDB accession code 1A07) and HLA-A2 (bottom right). For greater clarity, the α 3 and β 2m domains of HLA-Cw3 and HLA-A2 are not shown. The binding regions (intermolecular contact ≤ 4 Å) are depicted by molecular surface representations, coloured according to contact regions as labelled. GAV and Tax peptide residues that do not interact with KIR2DL2 or the A6 TCR, respectively, are shown as purple stick models. **c**, Structure-

based sequence alignments of the binding regions of KIR2DL2 and HLA-Cw3 with selected KIR receptors and class I MHCs. The sequence of KIR2DL3 is not shown because all six binding loops are identical to those of KIR2DL2. HLA-B2705 and HLA-B0801 are representative of Bw4 and Bw6 serotypes, respectively. Conserved residues are indicated by dashes. Helices are denoted by blue spirals. KIR residues that align with KIR2DL2 contact residues are blue on a green background. MHC residues that align with HLA-Cw3 contact residues are red on a yellow background. Red and blue dots at the bottom indicate MHC residues that interact with TCR in the HLA-A2/Tax/A6 TCR and H-2K^b/dEV8/2C TCR complexes, respectively.

conformation, Leu 7 of GAV is oriented upward, away from HLA-Cw3 and contacts KIR2DL2. Surface accessibility calculations indicate that the P7 position is normally 60–90% buried in the MHC peptide-binding cleft (Fig. 4b). In comparison, Leu 7 of GAV is only 38% buried in the HLA-Cw3 peptide-binding cleft despite being a hydrophobic residue. In marked contrast, the P7 position of HLA-Cw4 is completely buried¹⁴. These results indicate that the P7 of GAV may be hyperexposed relative to other class I MHC peptides at this position. Possibly, the interaction of KIR2DL2 with HLA-Cw3 induces a conformational change at the P7 position of GAV, resulting in the exposure of Leu 7 to KIR. It should be noted, however, that the peptide conformation of Leu 7 in the absence of KIR2DL2, is not known. In the complex, the side chain of leucine at P7 packs against Leu 104 and Tyr 105 of KIR, but this packing leaves sufficient space to accommodate different amino acids, such as tyrosine in the TAM peptide (Table 3). A similar change in peptide conformation involving position P7 was observed when the A6 TCR/HLA-A2/Tax complex was compared with the structure of HLA-A2/Tax alone²¹.

KIR binding imposes the peptide preference at position P8

The peptide contribution to the HLA-Cw4 allotype recognition by KIR2DL1 is limited to the P7 and P8 positions²²; however, the peptide preference for KIR2DL2/HLA-Cw3 recognition is less defined. In the complex structure, in addition to the hydrogen bond between the amide nitrogen of Ala 8 and Gln 71, Ala 8 is also surrounded by KIR residues Lys 44, Ser 184 and Asp 187. The particularly close proximity of Gln 71 substantially restricts the residue size at the P8 position, leaving little room to accommodate a side chain larger than valine or threonine. To examine further the P8 position size requirement, we used SPR techniques to measure the affinity of several variations of the GAV peptide with serine,

valine, lysine and tyrosine substitutions at position P8 (Table 3). Analysis of the binding of KIR2DL2 to HLA-Cw3 molecules refolded with these variant peptides revealed rapid kinetics ($k_{on} > 10^4 M^{-1} s^{-1}$ and $k_{off} > 0.5 s^{-1}$), consistent with previous SPR studies of KIR2D/HLA-C recognition^{23,24}. In general, KIR/HLA-C interaction has kinetics that are characteristic of low-affinity adhesion molecules, such as CD2 and CD58 (ref. 25), but that are faster than the kinetics of TCR/MHC interaction²⁴. Whereas all peptide variants of HLA-Cw3 bind to the class I specific antibody W6/32 with nearly equal affinity, their binding affinities for KIR2DL2 differ markedly (Table 3). Small amino acids like alanine and serine at the P8 position bound well to the receptor, whereas larger amino acids such as tyrosine and lysine essentially abolished binding to KIR. The binding of HLA-Cw3 with a motif peptide AAADAAAAL to KIR2DL2 was slightly lower than those of the alanine and serine variants but much better than the valine and tyrosine variants, suggesting that although other positions contribute to KIR recognition they are less critical than the P8 position.

Allotype specificity of KIR/HLA recognition

A primary difference between the KIRs and TCRs in MHC recognition is in the nature of peptide and MHC specificity. T-cell receptors are often restricted to a particular MHC allele and its peptide, but KIR recognition of class I MHC is mainly allotype specific. Peptide tolerance of KIR recognition is evident from the fact that only the P7 and P8 positions of the peptide contact the receptor, and P4, P5 and P6 positions make no contact with the receptor. KIR2DL2 buries ~36% of the exposed peptide surface of HLA-Cw3/GAV. In comparison, ~80% of the HLA-A2/Tax and the H-2K^b/dEV8 peptide surfaces are buried upon binding to their respective A6 and 2C TCRs (Fig. 3b). The low contribution of peptide to KIR2DL2/HLA-Cw3 interaction relative to that of TCR/MHC class I interaction renders KIR less sensitive to the identity of the peptides.

The basis for the MHC allotypic recognition of KIR is reflected in the composition of the KIR/HLA interface. Of the 12 HLA-Cw3 residues in the interface with KIR, 11 are invariant in all HLA-C alleles (Fig. 3c). In contrast, only 8 out of 16 residues of HLA-A2 in the A6 TCR interface are invariant in HLA-A alleles. Thus, KIR recognition of HLA-C alleles relies more on conserved residues relative to TCRs that interact with more polymorphic residues. Of particular interest is residue 80 of HLA-C which varies between asparagine in KIR2DL2-recognizing HLA-Cw1, 3, 7 and 8, and lysine in KIR2DL2-recognizing HLA-Cw2, 4, 5, 6 and 15 (ref. 26). Of the 16 KIR residues that contribute to the KIR/HLA interface, all are invariant in KIR2DL2 and 2DL3, and 14 are identical in 2DL1 (Fig. 3c). Only two residues differ between KIR2DL2 and 2DL1—Lys 44 and Met 70 in 2DL2, and Met 44 and Thr 70 in 2DL1. The high degree of sequence conservation of the interface residues on both KIR and HLA-C suggests a common binding mode for the KIR2DL1, 2DL2 and 2DL3 receptors. Residue 44 of KIR and residue 80 of HLA-C have been implicated as critical residues in defining allotype specificity^{12,27}. Indeed, Lys 44 of KIR2DL2 forms a hydrogen

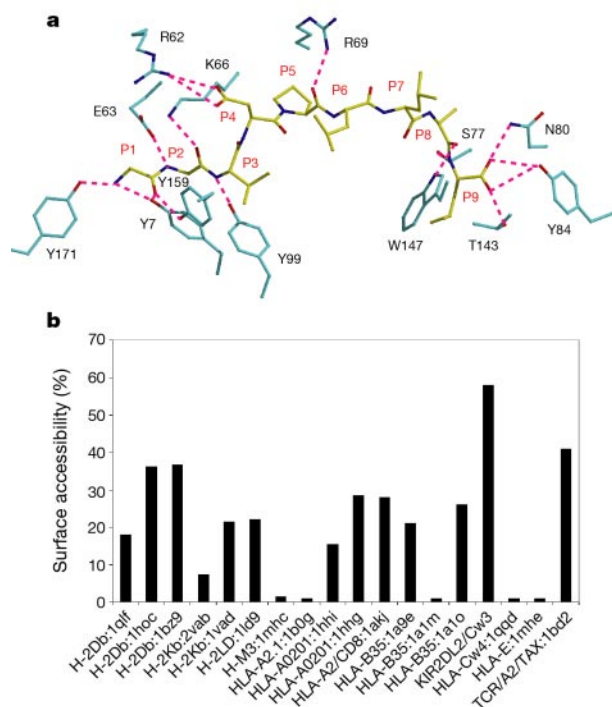


Figure 4 Coordination of the GAV peptide. **a**, Stick model showing the hydrogen-bonding pattern (dotted lines) between HLA-Cw3 (cyan) and the GAV peptide (yellow).

b, Percentage peptide surface accessibility at peptide position P7. The survey includes nonamer peptide–MHC class I molecule structures deposited in the Protein Data Bank (codes are given along the abscissa). In the case of KIR/MHC and TCR/MHC complexes, the calculation was done without the presence of the receptors.

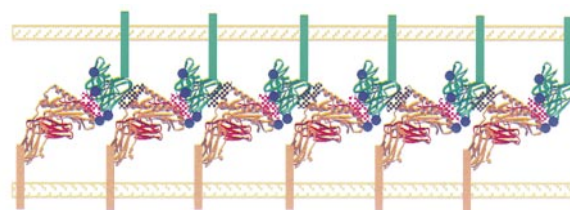


Figure 5 KIR/HLA aggregation. The complex of KIR2DL2 and HLA-Cw3 forms a regular oligomeric aggregate in the crystal lattice. KIR and HLA-Cw3 are shown in green and orange, respectively. The functional and oligomeric KIR/HLA-Cw3 interfaces are highlighted in pink and grey, respectively. The predicted glycosylation sites (highlighted by blue dots) are at residues 63, 157 and 190 for KIR, and at 86 for HLA-Cw3.

bond with Asn 80 of HLA-Cw3 in the complex structure. This hydrogen bond would have been lost when either Lys 44 of KIR2DL2 was replaced with methionine, as in KIR2DL1, or Asn 80 was replaced with lysine, as in the HLA-Cw2, 4, 5, 6 and 15 allotypes. Indeed, the K44M mutation of KIR2DL2 causes complete loss of the HLA-Cw3 binding (Table 3). Thus, one hydrogen bond preferentially stabilizes the KIR2DL2/HLA-Cw3 pair over both 2DL1/HLA-Cw3 and 2DL2/HLA-Cw4 pairs and is sufficient in determining the receptor–ligand specificity. The result of K44M mutation further supports the notion that the threshold of KIR/HLA recognition is high and the recognition is intolerant to interface mutations.

The three-domain receptor, KIR3DL1, binds to HLA-B alleles, specifically the Bw4 serotype. A comparison with HLA-B alleles reveals that all but three of the interface residues (Arg 69, Val 76 and Asn 80) are conserved across HLA-B and HLA-C loci (Fig. 3c). In HLA-B alleles, position 69 is an alanine or threonine, position 76 is a glutamic acid and position 80 is an asparagine, threonine or isoleucine. These three residues may determine locus specificity between HLA-B and HLA-C alleles. Indeed, HLA-B46, an unusual B allele that has HLA-Cw1 residues in positions 66–76, inhibits NK cells with HLA-Cw1 specificity²⁸. Nine of the sixteen KIR2DL2 interface residues are conserved in the second and third extracellular domains of KIR3DL1 (Fig. 3c). Moreover, peptide position P7 and P8 are also important for NK cell recognition of HLA-B2705 (ref. 29). Although the D0 domain of KIR3DL1 is also required for ligand recognition³⁰, the above observations suggest that KIR3DL1/HLA-Bw4 interaction is similar to that of KIR2DL2/HLA-Cw3.

The structure of a murine C-type lectin-like NK receptor Ly49A in complex with its class I MHC ligand, H-2D^d has been determined¹⁰. Although both KIR2DL2/HLA-Cw3 and Ly49A/H-2D^d recognition are dominated by charge–charge interactions, they bind to opposite ends of the class I molecule with direct peptide contact observed with KIR, but not with Ly49A. The binding of class I by KIR is, in fact, more similar to that of the TCR than to that of Ly49A. The differences between TCR, KIR and Ly49A in their recognition of class I MHC molecules illustrate both the multiplicity and complexity of the immune system.

Ligand-induced receptor aggregation

This structure and previous solution studies²⁴ suggest a 1:1 stoichiometry for KIR/HLA interaction. It is not yet clear how the signal transduction machinery detects the engagement of KIR by class I, but the formation of ligand-induced higher order oligomers is a likely mechanism. Within the KIR/HLA complex crystal and apart from the binding interface, the first KIR molecule (KIR A) also makes an additional contact with a translationally related HLA-Cw3 in a peptide-independent manner. This interaction forms an oligomeric KIR/HLA aggregate, linking adjacent pairs of complexes in the same orientation that also maintains the 1:1 molar ratio between KIR and HLA (Fig. 5). The contact surface is formed between the B and E β -strands of the KIR D2 domain and the C-terminal end of the α 2 helix of HLA-Cw3 (Fig. 5). This interface buries 528 Å² of surface area and is characterized by mostly van der Waals interactions. The putative glycosylation sites on both KIR2DL2 and HLA-Cw3 are outside this oligomeric KIR/HLA interface. It is possible that this form of receptor–ligand oligomerization resembles the receptor clustering on the surface of NK cells during immune synapse formation. However, further studies are needed to address the biological relevance of this oligomeric form, particularly its implication for receptor signalling.

Shared recognition between KIR and TCR

As part of the immunosurveillance system, classical class I MHC molecules present foreign peptides to cytotoxic T-cells through TCRs, thereby eliciting T-cell responses. The very same MHC

molecules can also present self peptides to NK cells through inhibitory KIR receptors in the absence of foreign peptides and thereby confer protection of healthy cells against NK-directed cytotoxicity. Whether KIR receptors preferentially recognize a pool of peptides distinct from those recognized by TCR is not clear. In the case of inhibitory receptors, however, it may be beneficial if such recognition of foreign peptides by KIR were less stable than the self-recognition by KIR. CD8 positive T cells that are reactive against HLA-Cw3 containing the HIV gag peptide QAISPRTL have been identified³¹. This octameric peptide has a threonine at the P Ω -1 position and a fivefold reduced affinity for KIR2DL2 relative to GAV when complexed with HLA-Cw3 (Table 3). An HLA-Cw4 restricted T-cell epitope peptide has been shown not to be recognized by KIR2DL1 (ref. 22); it is therefore possible that KIR receptors may be optimized to bind to MHC with self peptides. The situation may, however, be different in murine system where the Ly49 family of receptors appears less sensitive to the peptide identity^{32,33}.

This work provides the first structural insight to KIR/HLA recognition, but many questions remain unanswered. What is the structural role of zinc ion in KIR receptor function and what is the structural organization of the NK cell immune synapse^{34,35}? Does KIR3D recognition of HLA-B alleles share the same structural features predicted from the KIR2DL2/HLA-Cw3 interface? Further structural work is needed to address these questions and to allow us to understand better the machinery of innate immune recognition. □

Methods

Protein expression, purification and crystallization

KIR2DL2 was expressed and purified as described⁷. The heavy chain of HLA-Cw304 (1–278) and β 2m (0–99) were expressed separately as *Escherichia coli* inclusion bodies and then reconstituted *in vitro* together with the peptide GAVDPLAL, purified on a Source Q anion exchange column and a Superdex 200 gel-filtration column. The complex of KIR2DL2 and HLA-Cw3 was prepared by mixing both components in a 1:1 molar ratio. Crystals were grown at room temperature by hanging drop vapour diffusion methods to 0.05 × 0.1 × 0.4 mm in size using 6% PEG 20,000, 50 mM CaCl₂ and 50 mM sodium cacodylate at pH 6.5 and 10 mg ml⁻¹ of the complex.

Structure determination

All data were collected at –180 °C using an ADSC Quantum IV CCD detector on the X9B beam line of the National Synchrotron Light Source (NSLS) at the Brookhaven National Laboratory and processed using HKL2000 (ref. 36). Before freezing, crystals were soaked briefly in precipitant solution containing 25% glycerol. The crystals diffract to 3.0 Å resolution and belong to the orthorhombic space group P2₁2₁2₁ with unit-cell dimensions of $a = 68.5$, $b = 90.3$ and $c = 207.3$ Å. There are one HLA-Cw3/GAV peptide and two KIR2DL2 molecules in the asymmetric unit.

The structures of HLA-Cw3 and both KIR2DL2 molecules were determined by molecular replacement using the program AmoRe³⁷. The polyaniline version of HLA-A2 (PDB accession number 1B0G) was used as the model in rotation and translation searches using 10–3.5 Å data. This yielded a clear solution with a correlation coefficient of 40.0% and an R factor of 53.8%. After rigid body refinement of individual domains using the program CNS³⁸, most side chains of HLA-Cw3 had clear electron density into which all but 40 side chains were built. The first KIR2DL2 molecule was identified by a search using a polyaniline model of the unbound KIR2DL2 (PDB accession code 2DL2) as a model and with the HLA-Cw3 position fixed. The solution had a correlation coefficient of 44.1% and an R factor of 51.0%. After preliminary refinement in CNS, a second KIR molecule was visible in the $F_o - F_c$ map contoured to 2.0 σ and its position was defined by further searches using the fixed positions of HLA-Cw3 and the first KIR. This yielded a final solution with a correlation coefficient of 66.6% and an R factor of 40.1%.

Positional and grouped B -factor refinement was carried out using the maximum likelihood method of CNS including a bulk-solvent correction and anisotropic B -factor scaling of F_o in conjunction with remodelling using the program O (ref. 39). Reflections from 10.0 to 3.0 Å with $F_o \geq 1.0\sigma_{F_o}$ were used for refinement, excluding 5% that were used for R_{free} calculations. Non-crystallographic symmetry (NCS) restraints of 75 kcal mol⁻¹ were imposed between KIR A and KIR B. Water molecules were added manually using $F_o - F_c$ electron density maps contoured at 3.0 σ . The final model includes residues 1–278 of HLA-Cw3, 0–99 of β 2m, 4–200 for both KIR molecules and all 9 residues of the peptide GAVDPLAL.

Structural analysis

Buried surface area calculations were performed with the program SURFACE⁴⁰ using a probe radius of 1.4 Å. Shape correlation statistics were determined using the program SC¹⁵. The hinge angle between various domains was determined using the program HINGE

(P.S., unpublished), which calculates the angle between vectors representing the principal moment of inertia for polyaniline models of each domain. The residues used for calculating the hinge angles are 4–103 and 107–200, respectively, for the KIR D1 and D2 domains, and 1–182 and 183–275, respectively, for the MHC $\alpha 1\alpha 2$ and $\alpha 3$ domains. The docking angle between KIR2DL2 and HLA-Cw3 was calculated using residues 4–200 of KIR2DL2 and 1–182 of HLA-Cw3.

SPR and analytical ultracentrifugation measurements

HLA-Cw3 was reconstituted in the presence of individual peptides as listed in Table 3. SPR measurements were performed using a BIAcore 2000 instrument (BIAcore AB). Either soluble KIR2DL2 receptor (0.1 mg ml^{-1}) or a class I MHC specific monoclonal antibody w6/32 (0.04 mg ml^{-1}) were immobilized on a CM5 sensor chip at pH 6.0 with *N*-hydrosuccinimide / 1-ethyl-3-(3-dimethylaminopropyl)-carbodiimide hydrochloride (NHS/EDC). Immobilization of the receptor was assessed by the binding of the KIR2DL2 blocking antibody GL183 (Coulter Corp) and the integrity of refolded HLA-Cw3 was assessed by the binding of HLA-Cw3 to w6/32. The binding of HLA-Cw3 to immobilized KIR2DL2 was measured using serial dilutions of HLA from 0.3 to $40 \mu\text{M}$ at a flow rate of $5 \mu\text{l min}^{-1}$ without regeneration of the chip. HLA-E was used as a negative control. The dissociation constants (K_d) were obtained from the steady-state curve fitting analysis using BIAevaluation 3.0 (BIAcore AB) or linear regression using ORIGIN 3.0 (MicroCal Software, Inc.).

Sedimentation equilibrium profiles were obtained in a Beckman XL-A at rotor speeds of 20K, 28K and 35K r.p.m. Samples with varying concentrations of HLA-Cw3 and KIR2DL2 in 20 mM sodium cacodylate and 20 mM CaCl_2 were used. All components were well described by thermodynamically ideal monomeric species, with buoyant molar masses consistent with those calculated from the amino-acid sequence. Data was analysed by a global fit of several equilibrium distributions at multiple rotor speeds, protein concentrations and molar ratios.

Generation of mutant KIR

A complementary DNA encoding residues 1–200 of KIR2DL2 was subcloned into pET30BirA allowing in-frame fusion of a sequence encoding the substrate for BirA. KIR mutations were then generated using a DNA QuikChange Kit (Stratagene) and plasmids containing the desired mutations were identified by automated sequencing.

Received 24 January; accepted 4 April 2000.

- Biron, C. A., Nguyen, K. B., Pien, G. C., Cousens, L. P. & Salazar-Mather, T. P. Natural killer cells in antiviral defense: function and regulation by innate cytokines. *Annu. Rev. Immunol.* **17**, 189–220 (1999).
- Lanier, L. L. NK cell receptors. *Annu. Rev. Immunol.* **16**, 359–393 (1998).
- Lanier, L. L., Corliss, B. C., Wu, J., Leong, C. & Phillips, J. H. Immunoreceptor DAP12 bearing a tyrosine-based activation motif is involved in activating NK cells. *Nature* **391**, 703–707 (1998).
- Long, E. O. Regulation of immune responses through inhibitory receptors. *Annu. Rev. Immunol.* **17**, 875–904 (1999).
- Pende, D. *et al.* The susceptibility to natural killer cell-mediated lysis of HLA class I-positive melanomas reflects the expression of insufficient amounts of different HLA class I alleles. *Eur. J. Immunol.* **28**, 2384–2394 (1998).
- Fan, Q. R. *et al.* Structure of the inhibitory receptor for human natural killer cells resembles haematopoietic receptors. *Nature* **389**, 96–100 (1997).
- Snyder, G. A., Brooks, A. G. & Sun, P. D. Crystal structure of the HLA-Cw3 allotype-specific killer cell inhibitory receptor KIR2DL2. *Proc. Natl Acad. Sci. USA* **96**, 3864–3869 (1999).
- Maenaka, K., Juji, T., Stuart, D. I. & Jones, E. Y. Crystal structure of the human p58 killer cell inhibitory receptor (KIR2DL3) specific for HLA-Cw3-related MHC class I. *Structure* **7**, 391–398 (1999).
- Boyington, J. C. *et al.* Structure of CD94 reveals a novel C-type lectin fold: implications for the NK cell-associated CD94/NG2 receptors. *Immunity* **10**, 75–82 (1999).
- Tormo, J., Natarajan, K., Margulies, D. H. & Mariuzza, R. A. Crystal structure of a lectin-like natural killer cell receptor bound to its MHC class I ligand. *Nature* **402**, 623–631 (1999).
- Winter, C. C., Gumperz, J. E., Parham, P., Long, E. O. & Wagtmann, N. Direct binding and functional transfer of NK cell inhibitory receptors reveal novel patterns of HLA-C allotype recognition. *J. Immunol.* **161**, 571–577 (1998).
- Winter, C. C. & Long, E. O. A single amino acid in the p58 killer cell inhibitory receptor controls the ability of natural killer cells to discriminate between the two groups of HLA-C allotypes. *J. Immunol.* **158**, 4026–4028 (1997).
- Biassoni, R. *et al.* Role of amino acid position 70 in the binding affinity of p50.1 and p58.1 receptors for HLA-Cw4 molecules. *Eur. J. Immunol.* **27**, 3095–3099 (1997).
- Fan, Q. R. & Wiley, D. C. Structure of human histocompatibility leukocyte antigen (HLA)-Cw4, a ligand for the KIR2D natural killer cell inhibitory receptor. *J. Exp. Med.* **190**, 113–123 (1999).
- Lawrence, M. C. & Colman, P. M. Shape complementarity at protein/protein interfaces. *J. Mol. Biol.* **234**, 946–950 (1993).
- Ysern, X., Li, H. & Mariuzza, R. A. Imperfect interfaces. *Nature Struct. Biol.* **5**, 412–414 (1998).
- Wang, J. H. *et al.* Structure of a heterophilic adhesion complex between the human CD2 and CD58 (LFA-3) counterreceptors. *Cell* **97**, 791–803 (1999).
- Mandelboim, O. *et al.* The binding site of NK receptors on HLA-C molecules. *Immunity* **6**, 341–350 (1997).
- Zappacosta, F., Borrego, F., Brooks, A. G., Parker, K. C. & Coligan, J. E. Peptides isolated from HLA-Cw*0304 confer different degrees of protection from natural killer cell-mediated lysis. *Proc. Natl Acad. Sci. USA* **94**, 6313–6318 (1997).
- Falk, K. *et al.* Allele-specific peptide ligand motifs of HLA-C molecules. *Proc. Natl Acad. Sci. USA* **90**, 12005–12009 (1993).
- Garboczi, D. N. *et al.* Structure of the complex between human T-cell receptor, viral peptide and HLA-A2. *Nature* **384**, 134–141 (1996).
- Rajagopalan, S. & Long, E. O. The direct binding of a p58 killer cell inhibitory receptor to human histocompatibility leukocyte antigen (HLA)-Cw4 exhibits peptide selectivity. *J. Exp. Med.* **185**, 1523–1528 (1997).
- Vales-Gomez, M., Reyburn, H. T., Erskine, R. A. & Strominger, J. Differential binding to HLA-C of p50-activating and p58-inhibitory natural killer cell receptors. *Proc. Natl Acad. Sci. USA* **95**, 14326–14331 (1998).
- Maenaka, K. *et al.* Killer cell immunoglobulin receptors and T cell receptors bind peptide-major histocompatibility complex class I with distinct thermodynamic and kinetic properties. *J. Biol. Chem.* **274**, 28329–28334 (1999).
- Davis, S. J., Ikemizu, S., Wild, M. K. & van der Merwe, P. A. CD2 and the nature of protein interactions mediating cell-cell recognition. *Immunol. Rev.* **163**, 217–236 (1998).
- Colonna, M., Borsellino, G., Falco, M., Ferrara, G. B. & Strominger, J. L. HLA-C is the inhibitory ligand that determines dominant resistance to lysis by NK1- and NK2-specific natural killer cells. *Proc. Natl Acad. Sci. USA* **90**, 12000–12004 (1993).
- Mandelboim, O. *et al.* Protection from lysis by natural killer cells of group 1 and 2 specificity is mediated by residue 80 in human histocompatibility leukocyte antigen C alleles and also occurs with empty major histocompatibility complex molecules. *J. Exp. Med.* **184**, 913–922 (1996).
- Barber, L. D. *et al.* The inter-locus recombinant HLA-B*4601 has high selectivity in peptide binding and functions characteristic of HLA-C. *J. Exp. Med.* **184**, 735–740 (1996).
- Peruzzi, M., Parker, K. C., Long, E. O. & Malnati, M. S. Peptide sequence requirements for the recognition of HLA-B*2705 by specific natural killer cells. *J. Immunol.* **157**, 3350–3356 (1996).
- Rojas, S., Wagtmann, N. & Long, E. O. Binding of a soluble p70 killer cell inhibitory receptor to HLA-B*5101: requirement for all three p70 immunoglobulin domains. *Eur. J. Immunol.* **27**, 568–571 (1997).
- Littau, R. A. *et al.* An HLA-C-restricted CD8+ cytotoxic T-lymphocyte clone recognizes a highly conserved epitope on human immunodeficiency virus type 1 gag. *J. Virol.* **65**, 4051–4056 (1991).
- Hanke, T. *et al.* Direct assessment of MHC class I binding by seven Ly49 inhibitory NK cell receptors. *Immunity* **11**, 67–77 (1999).
- Orihuela, M., Margulies, D. H. & Yokoyama, W. M. The natural killer cell receptor Ly-49A recognizes a peptide-induced conformational determinant on its major histocompatibility complex class I ligand. *Proc. Natl Acad. Sci. USA* **93**, 11792–11797 (1996).
- Rajagopalan, S., Winter, C. C., Wagtmann, N. & Long, E. O. The Ig-related killer cell inhibitory receptor binds zinc and requires zinc for recognition of HLA-C on target cells. *J. Immunol.* **155**, 4143–4146 (1995).
- Davis, D. M. *et al.* The human natural killer cell immune synapse. *Proc. Natl Acad. Sci. USA* **96**, 15062–15067 (1999).
- Otwindowski, Z. & Minor, W. Processing of X-ray diffraction data collected in oscillation mode. *Methods Enzymol.* **276**, 307–326 (1997).
- Navaza, J. AMoRe: an automated package for molecular replacement. *Acta Crystallogr. A* **50**, 157–163 (1994).
- Brunger, A. T. *et al.* Crystallography & NMR system: A Software Suite for Macromolecular Structure Determination. *Acta Crystallogr. D* **54**, 905–921 (1998).
- Jones, T. A., Zou, J. Y., Cowan, S. W. & Kjeldgaard, M. Improved methods for building protein models in electron density maps and the location of errors in the models. *Acta Crystallogr. A* **47**, 110–119 (1991).
- The Collaborative Computing Project No. 4. The CCP4 suite: programs for protein crystallography. *Acta Crystallogr. D* **50**, 760–763 (1995).
- Kraulis, P. J. MOLSCRIPT: a program to produce both detailed and schematic plots of protein structures. *J. Applied Crystallography* **24**, 946–950 (1991).
- Merritt, E. A. & Murphy, M. E. P. Raster 3D Version 2.0: a program for photorealistic molecular graphics. *Acta Crystallogr. D* **50**, 869–873 (1994).
- Nicholls, A., Chapp, K. A. & Honig, B. Protein folding and association: insights from the interfacial and thermodynamic properties of hydrocarbons. *Proteins Struct. Funct. Genet.* **11**, 281–296 (1991).

Acknowledgements

We thank Z. Dauter and C. Titlow for help with synchrotron data collection; J. Lukszo for peptide synthesis; C. Hammer for mass spectroscopy measurements; M. Garfield for N-terminal amino-acid sequencing; A. Winterhalter and N. Mifsud for assistance with the mutagenesis and DNA sequencing; and D. Margulies for help with BIAcore SPR measurements. This work is supported by intramural research funding from the National Institute of Allergy and Infectious Diseases and an R. D. Wright Fellowship from the National Health and Medical Research Council, Australia.

Correspondence and requests for materials should be addressed to P.S. (e-mail: psun@nih.gov). Coordinates have been deposited in the Protein Data Bank under accession code 1EFX and are available before release from P.S.